JOINT INSTITUTE FOR AERONAUTICS AND ACOUSTICS

National Aeronautics and
Space Administration
Ames Research Center

JIAA TR - 92

Stanford University

TRANSPIRATION COOLING IN HYPERSONIC FLIGHT

BY

Domingo Tavella and Leonard Roberts

Stanford University
Department of Aeronautics and Astronautics
Stanford, CA 94305

NCC2-543

JUNE 1989

This research has been supported by NASA Grant NCC 2-543

ABSTRACT

A preliminary numerical study of transpiration cooling applied to a hypersonic configuration is presented. Air transpiration is applied to the NASA all-body configuration flying at an altitude of 30500 m with a Mach number of 10.3. It was found that the amount of heat disposal by convection is determined primarily by the local geometry of the aircraft for moderate rates of transpiration. This property implies that different areas of the aircraft where transpiration occurs interact weakly with each other. A methodology for quick assessments of the transpiration requirements for a given flight configuration is presented.

CONTENTS

NOMENCLATURE

c	constant of proportionality in transpiration intensity
C_p	pressure coefficient
C_μ	transpiration coefficient
h	enthalpy
k	constant of proportionality in transpiration intensity
M	Mach number
$\dot{q}$	heat flux
Re	Reynold's number
S	aircraft planform surface area
St	Stanton number
T	temperature
u	flow velocity
y	non-dimensional spanwise coordinate
ϵ	emissivity
γ	ratio of specific heats
ρ	fluid density
σ	Stefan-Boltzmann constant

Subscripts:

0	stagnation
a	aerodynamic
b	blowing
c	convective
n	conduction into aircraft
o	in the absence of transpiration
r	radiant
w	evaluated at wall
∞	evaluated at free stream

1. INTRODUCTION

The concept of transpiration cooling consists in allowing a gas - air, or, preferably a lighter gas such as helium - to transpire through porosity in the vehicle's skin. The transpired fluid alters the temperature gradient at the skin surface, thereby decreasing the heat transfer rate into the vehicle.

In hypersonic flight, the temperature of a non-transpiring surface results from the balance between heat radiated outward by the surface and heat conducted into the vehicle. In such cases the maximum temperature within the boundary layer is significantly higher than the vehicle's surface temperature. As a result, a strong temperature gradient exists at the surface. In a situation of thermal balance, the surface temperature will be such that the heat transfer due to this temperature gradient is entirely balanced by outward radiation.

In configurations intended for hypersonic flight, the skin temperature determined by radiation equilibrium may be significantly higher than can be withstood by the material of the skin. In this case, the skin temperature must be decreased by enhancing the depletion rate of the heat produced within the boundary layer. Transpiration brings this about through a large enthalpy change in the cooling medium as it emerges out of the porous skin and becomes an integral part of the boundary layer. In this manner, the heat that cannot be disposed of by radiation is absorbed by the coolant and convected by the boundary layer. Equivalently, the right amount of transpiration causes a suitable change in the temperature gradient at the skin, such that heat transferred to the wall will match that disposed of by thermal radiation.

In principle, the rate of transpiration required to dispose of a given amount of heat flux cannot be easily inferred. Transpiration itself, through its interaction with the boundary layer, alters the rate of heat production within the boundary layer. This implies that, in general, transpiration cooling constitutes a non-linear problem. For a sufficiently small amount of transpiration, however, transpiration blowing may exert a significant impact on the thermal boundary layer, without significantly disturbing the momentum of the boundary layer. In such a case, since the latter is responsible for the excess heat ultimately to be convected by the transpired fluid the problem becomes an essentially linear one. The implication would be that the amount of transpiration required to dispose of a given excess heat flux would be a function of surface position only.

Transpiration cooling has been treated extensively in the literature. This concept is classified as a particular case of "film cooling", which includes gas injection from slots, discrete holes, porous surfaces, etc. Ref. (1) contains an extensive survey of the literature on the subject up to the year 1985. Due to the nature of the problem and the absence of computational tools in the past, previous work in this areas has been primarily experimental[2]. However limited due to the complexity of the problem, theoretical work has provided insight in cases where similarity solutions can be established[3]. Semi-empirical methods have also been developed[1].

In this work, the impact of transpiration blowing on heat convection was studied numerically for a hypersonic configuration flying at Mach 10.3 at an altitude of 30500 m. Detailed scrutiny of the boundary layers was conducted, and the conditions where transpiration blowing becomes a local function of surface location were identified. A methodology to assess the blowing requirements from a very limited number of CFD computations was demonstrated.

2. HEAT TRANSFER BALANCE

2.1 Aerodynamic and Radiant Heating

The aerodynamic heating at a particular location on the aircraft skin is denoted by $\dot{q}_a$. This is defined as the heat flux produced within the boundary layer that is directed toward the surface. The aerodynamic heating is balanced by the heat conducted toward the interior of the skin, denoted by $\dot{q}_n$, by the heat radiated outward by the surface, indicated by $\dot{q}_r$, and, if mass transfer is present, by the heat flux convected by the coolant medium, $\dot{q}_c$, as shown in Fig. 1.

$$\dot{q}_a + \dot{q}_n = - (\dot{q}_r + \dot{q}_c) \tag{1}$$

The radiant heat is related to the skin temperature as follows

$$\dot{q}_r = \sigma \epsilon T_w^4 \tag{2}$$

where σ is the Stefan-Boltzmann constant and ϵ is the emissivity of the surface.
In the analysis that follows it will be assumed that thermal equilibrium exists, that is $\dot{q}_n = 0$.

In keeping with the convention found in the literature, this study will be conducted in terms of the non-dimensional form of the heat transfer known as Stanton number, defined as

$$St = \frac{\dot{q}}{\rho_\infty u_\infty (h_{0_\infty} - h_w)} \tag{3}$$

Eq. (1) now becomes

$$St_a = St_r + St_c \tag{4}$$

For a gas with constant Cp, the radiant Stanton number is

$$St_r = \frac{\sigma \epsilon T_w^4}{\rho_\infty u_\infty C_p (T_\infty - T_w)} \tag{5}$$

Rewriting Eq. (5) in terms of T_w/T_∞ and T_{0_∞}/T_∞ and introducing the Mach number, the radiant Stanton number becomes:

$$St_r = \frac{\sigma \epsilon}{M_\infty C_p \sqrt{C_p(\gamma-1)}} \frac{T_\infty^{2.5}}{\rho_\infty} \frac{\left[\frac{T_w}{T_\infty}\right]^4}{\left[1+\frac{\gamma-1}{2}M_\infty^2 - \frac{T_w}{T_\infty}\right]} \tag{6}$$

Fig. 2 shows the radiant Stanton number as a function of the skin temperature ratio for the case of interest here, $M_\infty = 10.3$ at an altitude of 30,500 m. The emissivity is assumed to be equal to one.

2.2 Sensitivity of Radiant Heat to Skin Temperature

In a situation of equilibrium, the amount of heat to be balanced by radiation equals the heat flux produced by aerodynamic heating. The computation of the aerodynamic heating requires knowledge of the wall temperature. As a result, the assessment of the skin temperature which balances the aerodynamic heating by radiation can only be accomplished through an iteration process. In this process the wall temperature is guessed, the aerodynamic heating is computed, the heat balanced is checked, the skin temperature is adjusted and the whole process is repeated until the heat balance is verified. When dealing with hypersonic flow computations, this process can become excessively expensive. The following approach drastically reduces or eliminates the need for iterations.

Assume the skin temperature to be in error by δT_w. Since the aerodynamic heating is driven by $T_{0_\infty} - T_w$, the aerodynamic heating would be in error by the amount

$$\frac{\delta St_a}{St} = - \frac{\delta T_w}{T_{0_\infty} - T_w} \tag{7}$$

Introducing the following approximation for high Mach number:

$$\frac{T_{0_\infty}}{T_\infty} \sim \frac{\gamma-1}{2} M_\infty^2 \tag{8}$$

Eq. (7) gives, with γ=1.4

$$\frac{\delta St_a}{St} = - \frac{\delta T_w}{T_w} \frac{T_w}{T_\infty} \frac{5}{M_\infty^2} \left[1 + \frac{5}{M_\infty^2} \frac{T_w}{T_\infty} \right] \tag{9}$$

In stratospheric flight and for skin materials of interest, $\frac{T_w}{T_\infty} \sim 7$. With this value and $M_\infty = 10.3$, Eq. (9) gives

$$\frac{\delta St}{St} \sim - 0.5 \frac{\delta T_w}{T_w} \tag{10}$$

The skin temperature readjustment needed to counteract this error in the Stanton number can now be explored. Calling this readjustment δT_w, we get from Eq. (5):

$$\frac{\delta St_r}{St_r} = \frac{\delta T_w^*}{T_w} \left[4 + \frac{T_w}{T_\infty} \frac{5}{M^2} (1 + \frac{5}{M^2} \frac{T_w}{T_\infty}) \right] \tag{11}$$

Equating Eqs (9) and (10)

$$\delta T_w^* \sim -0.1 \ \delta T_w \tag{11}$$

This indicates that an iteration scheme would impart corrections to the skin temperature which decrease by an order of magnitude at each step. Under these conditions, a small relative change in the wall temperature has a small impact on the aerodynamic heating and a large impact on the radiant heat flux. This implies that if one has a reasonably good first estimate of the skin temperature, no additional corrections would be needed. Very minor adjustments of the skin temperature will allow for the disposal of a desired fraction of the heat by radiation. For a given Mach number, this

fact becomes more marked as the skin temperature ratio increases. These observations are particularly true in the case of transpiration blowing, where only part of the aerodynamic heating is to be disposed of by radiation.

3. NUMERICAL COMPUTATIONS

3.1 Algorithm and CFD Code

The three-dimensional thin-layer Navier-Stokes equations are solved with the finite difference algorithm developed by Fujii and Obayashi[4], including an upwind formulation later developed by Obayashi[5]. Features and implementation of the algorithm have been discussed elsewhere and will not be repeated here[5,6]. Difficulties in achieving stability lead to the utilization of a spatially first-order version of the upwind algorithm.

3.2 Hypersonic Configuration

The computations were conducted for the NASA Ames all-body hypersonic configuration, shown schematically in Fig. (3). All physical lengths were non-dimensionalized with the chord length. The computational grid, shown in Fig. (4), was generated by a hyperbolic grid generator. The grid size was 33 points in the streamwise direction, 49 points in the circumferential direction and 32 points in the radial direction, which amounted to a total number of grid points of 51744. Details of the grid generation are presented in Ref. 6.

3.3 Computational Performance

The computations were carried out on the CRAY XMP 48 supercomputer at NASA Ames Research Center. The computations were carried out in a non-time-accurate fashion. The number of iterations required for convergence before the onset of transpiration was about 5000 at Mach number 10.3, with a Reynolds number of 5,000,000 and an angle of attack of 15 degrees. Transpiration cooling was simulated numerically by implementing suitable boundary conditions and by utilizing a converged solution in the absence of transpiration as a starting computational solution. A further 4000 iterations were required after the onset of transpiration. The high number of

iterations is attributed to the extreme stiffness of the equations at hypersonic speeds and the corresponding need for very small local time steps in the vicinity of the body surface. Convergence time after blowing is started is limited by speed of convection of the injected fluid into the boundary layer. Such convection occurs very slowly, due both to the small time steps and the relatively low velocities within the boundary layer.

3.4 Transpiration Implementation

Transpiration is implemented by modifying the boundary conditions at the body surface. The normal mass flux at the body surface is defined locally as follows:

$$\rho_b u_b = k \frac{\dot{q}_0}{h_{0_w} - h_w} \tag{1}$$

with u_b normal to the body surface. This representation of blowing in terms of a constant k and of $\dot{q}_0$, the heat transfer in the absence of transpiration, has definite advantages, as will be shown below. Non-dimensionalizing with respect to $\rho_\infty u_\infty$ gives

$$\bar{\rho}_b \bar{u}_b = k \, St_0 \tag{2}$$

The analysis was based on information extracted from only two blowing configurations, shown in Figs. (5a) and (5b): Transpiration over the entire lower surface of the body for k = 0.25, 0.5, and 1.0, and transpiration over the lower surface corresponding to the outer 17% of the span for k = 0.25.

3.5 Flow Field Computations

In order to assess the impact of transpiration on the external aerodynamics of the vehicle, a detailed observation of the flow field was conducted. Figs. (6a) through (6d) show pressure

contours in the absence of transpiration at various chordwise stations of the body. The presence of a bow shock near the lower surface is clearly visible. Figs. (7a) and (7b) show pressure contours for the cases without transpiration and with transpiration corresponding to $k = 0.25$ for the configuration of Fig. (5b). Very slight differences can be observed. Since pressure contours are extremely sensitive indicators of flow field configurations, it may be concluded that transpiration blowing does not alter the external aerodynamics to any considerable extent.

Further insight into the effect of transpiration blowing on the flow field about the aircraft can be gained from observing the thermal and velocity boundary layers. This is illustrated in Figs. (8a) and (8b) for the blowing configuration of Fig. (5b). In both cases, the vertical axis represents the distance along the normal to the surface.

Fig. (8a) shows the thermal boundary layer at the hottest spot of the 50%-chord cross-section, which occurs at 98% of the span on the lower surface. As a result of transpiration, the sharp peak in the temperature distribution becomes blunter and is altered in a way that the normal temperature gradient at the surface is lower. Fig. (8b) shows the velocity boundary layer, where the variable represented is the modulus of the velocity. Transpiration has the effect of causing a slight swelling of the velocity profile. This slight swelling corresponds to a very small increment in the displacement thickness of the boundary layer as a result of transpiration. In its turn, this small increment in displacement thickness causes the very slight changes that can be perceived in the pressure contour plots of Figs. (7a) and (7b).

4. HEAT TRANSFER ASSESSMENT

4.1 Local Effect of Transpiration Cooling

Figs. (9a) and (9b) show the spanwise heat transfer distribution for the configurations of Figs. (7a) and (7b) respectively, for various values of transpiration intensity. As expected, the effect of transpiration is most noticeable on the lower surface of the body. Detailed observation of Figs. (9a) and (9b) indicates that the effect of blowing on heat transfer is, to a reasonable approximation, dependent on the local geometry only. This is shown in Fig. 10, where the ratio $-St_c/(St_a-St_c)$ has been plotted against various values of k for different locations along the span. For moderate transpiration intensities, the following relationship appears to hold:

$$\frac{-St_c}{St_a-St_c} = ck \tag{1}$$

where the constant c depends on the spanwise location. Notice that in the region where aerodynamic heating is most severe, this linearity appears to extend to values of k of at least 1. Furthermore, the information extracted from Fig. 9b indicates that the constant of proportionality in Eq. (1) may plausibly be assumed to be independent of transpiration distribution. Even though this may be only a rough approximation, it can be exploited to great advantage in conducting a preliminary assessment of transpiration requirements without the need for extensive computations.

Denoting the heat transfer rate under transpiration by q, Eq. (1) can also be written as follows:

$$\frac{\dot{q}}{\dot{q}_0} = \frac{1}{1+c\dfrac{\rho_b u_u (h_{0_w}-h_w)}{\dot{q}_0}} \tag{2}$$

4.2 Transpiration Intensity Assessment

The skin temperature at a particular point will be lower than a desired value T_w if the heat locally dissipated by radiation exceeds or equals the aerodynamic heating at that particular point. Blowing is applied to regions of the skin where this is not the case in a amount such that it causes the difference between the local aerodynamic and radiant heating rates to be eliminated by convection. In view of the analysis carried out in Chapter 2, this can be accomplished without any further computations by determining the values of constant c at the grid points on the body surface. Utilizing Eq. (1) with a value of St corresponding to desired radiation-balance heat transfer, a local value of k can be computed, which gives the local transpiration intensity when substituted in Eq. (3.2). This process is illustrated in Figs. 11, 12 and 13.

Fig. 11 shows the distribution of aerodynamic heat transfer for various cross-section of the body along the chord, for a wall temperature of 1366°K. The plot is made normally to the wing cross-sectional contour line. The dashed line represents the maximum level of heat transfer to be balanced by radiation. In this illustration, this value is 0.002, corresponding to a skin temperature of about 1400°K. The excess of heat transfer, represented by the area encompassed by the solid and dashed lines, is to be dissipated by transpiration. The jaggedness near the apex can be attributed to the spacial resolution of the numerical scheme being first order, while the computation of the heat transfer rates involves first order derivatives. Fig. 12 illustrates the required values of the constant k to cause such dissipation. The plot is done in a similar way, with the dashed line corresponding to k = 1 indicated as a reference. This was obtained by evaluating Eq. (1) at all grid points on the surface. Notice that the jaggedness near the apex has increased. This is caused by the ratio in Eq. (1), which tends to enhance the peaks and valleys of the jagged curve. Finally, Fig. 13 shows the local intensity of transpiration

per unit area needed to dissipate the aerodynamic heating in excess of St = 0.002 by convection. The dashed line is a reference and corresponds to a non-dimensional mass flow density of 0.005.
A transpiration coefficient is defined as follows:

$$C_m = \frac{\int \rho_b u_b dS}{\rho_e u_e S} \qquad (3)$$

where the integral extends over the area of the wing where blowing is applied, and S is the wing surface. The transpiration coefficient is represented in Figs. 14a and b for variable radiation level and corresponding skin temperature. For a vehicle with the shape of the NASA Ames all-body and an equilibrium skin temperature of 1600 °K, this analysis indicates that the blowing requirement amounts to approximately 0.03 Kg of air per square meter of planform surface area.

CONCLUSIONS

A preliminary analysis of transpiration cooling as a means to alleviate aerodynamic heating of a hypersonic configuration was conducted. It was found that the necessary mass flow rate to maintain radiation balance is approximately a local function of surface location, which leads to a simple process for estimating the transpiration requirements. The feasibility of this concept will depend on the allowable skin temperature.

REFERENCES

1. W.M. Rohsenow, J.P. Hartnett, and E.N. Ganie, Handbook of Heat Transfer Applications, McGraw-Hill Book Co., 1985.

2. L.W. Woodruff and G.C. Lorenz, "Hypersonic Turbulent Transpiration Cooling Including Downstream Effects," AIAA Journal, Vol. 4, No. 6, June 1966.

3. J.P. Hartnett and E.R.G. Eckert, "Mass-Transfer Cooling in a Laminar Boundary Layer with Constant Fluid Properties," Transactions of the ASME, pp. 247-254, February 1957.

4. K. Fujii and S. Obayashi, "Practical Applications of New LU-ADI Scheme for the Three-Dimensional Navier-Stokes Computations of Transonic Viscous Flows," AIAA Paper No. 86-0513, 1986.

5. S. Obayashi, "Numerical Simulation of Underexpanded Plumes Using Upwind Algorithms," AIAA Paper No. 88-4360 CP, AIAA Atmospheric Flight Mechanics Conference, Minneapolis, Minnesota, August 1988.

6. D. Yeh, D. Tavella, and L. Roberts, "Numerical Study of Delta Wing Leading Edge Blowing," JIAA TR-86, Stanford University, July 1988.

FIGURES

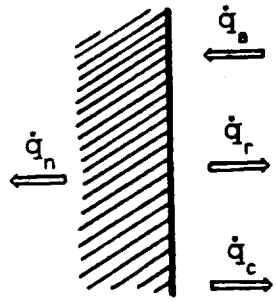

Fig. 1 Heat flux balance

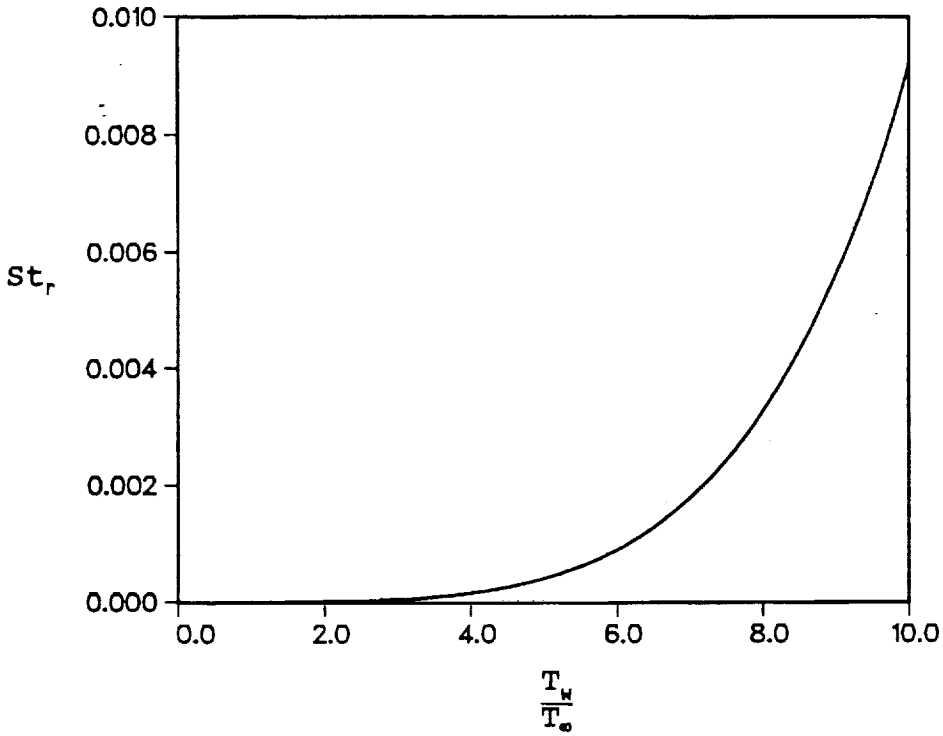

Fig. 2 Radiant Stanton number at 30,500 m, M = 10.3

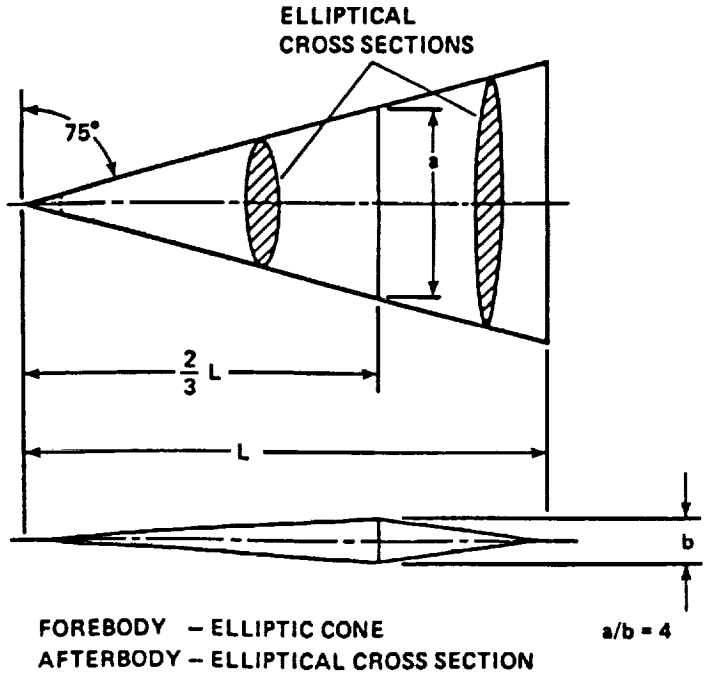

Fig. 3 All-body hypersonic configuration

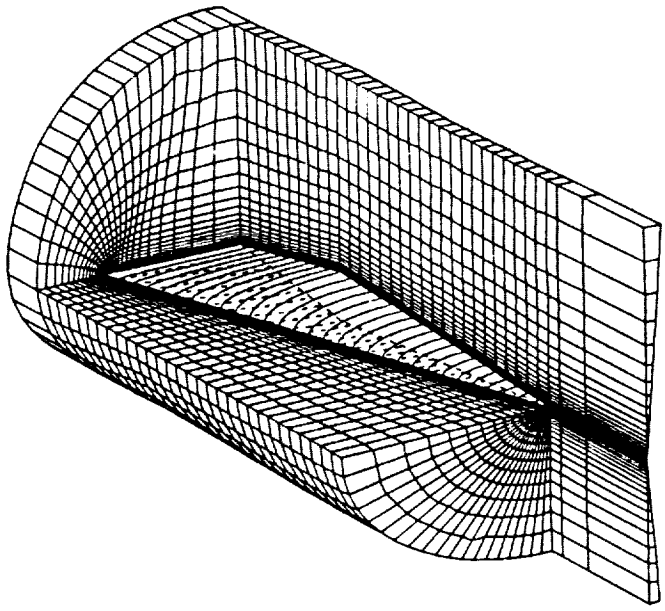

Fig. 4 Computational grid

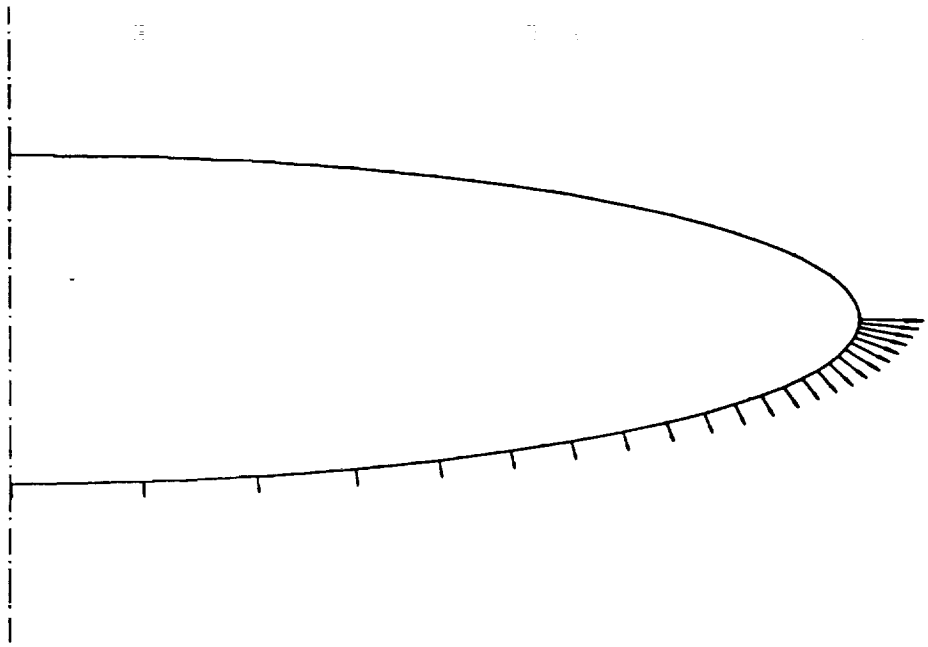

(a) Transpiration on entire lower surface

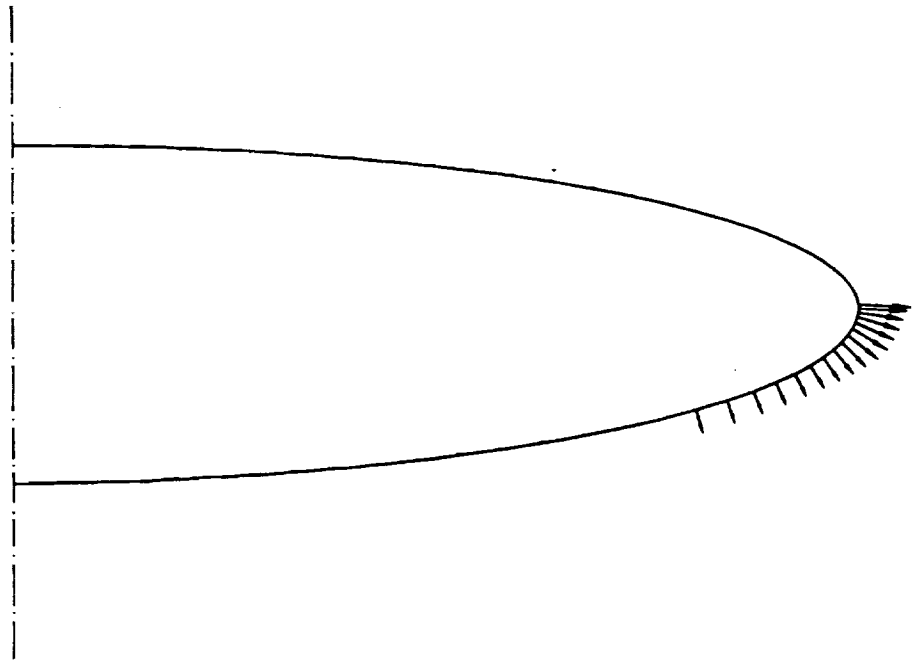

(b) Transpiration on outer 17% of span

Fig. 5 Transpiration blowing configurations

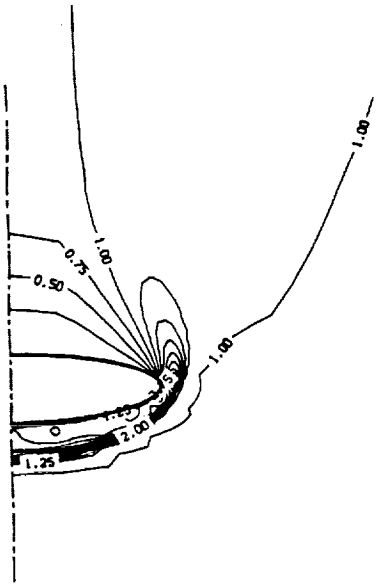

(a) 20% chord

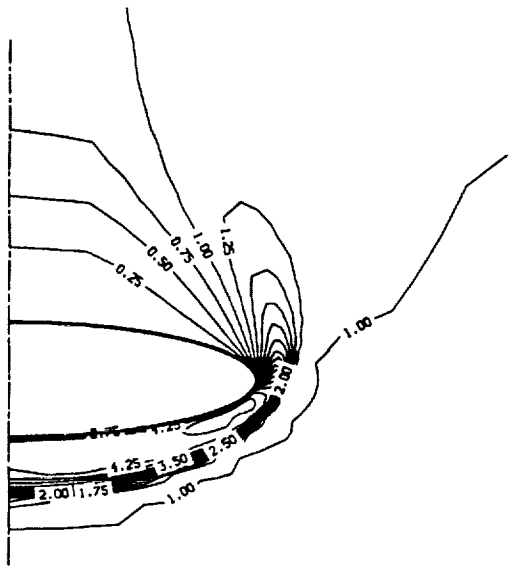

(b) 33% chord

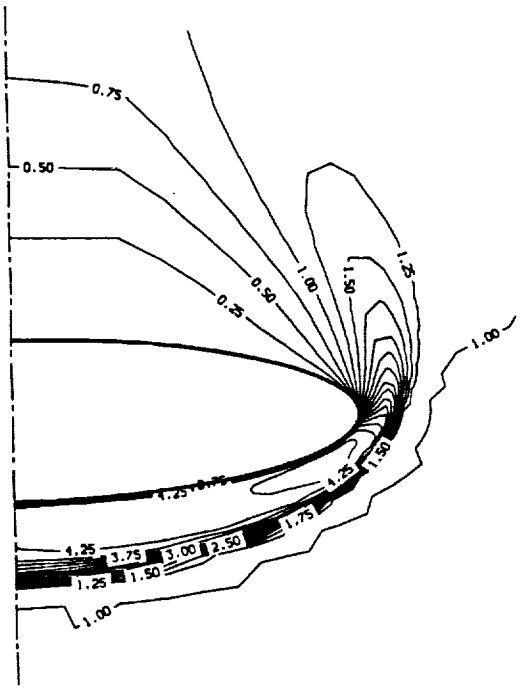

(c) 47% chord

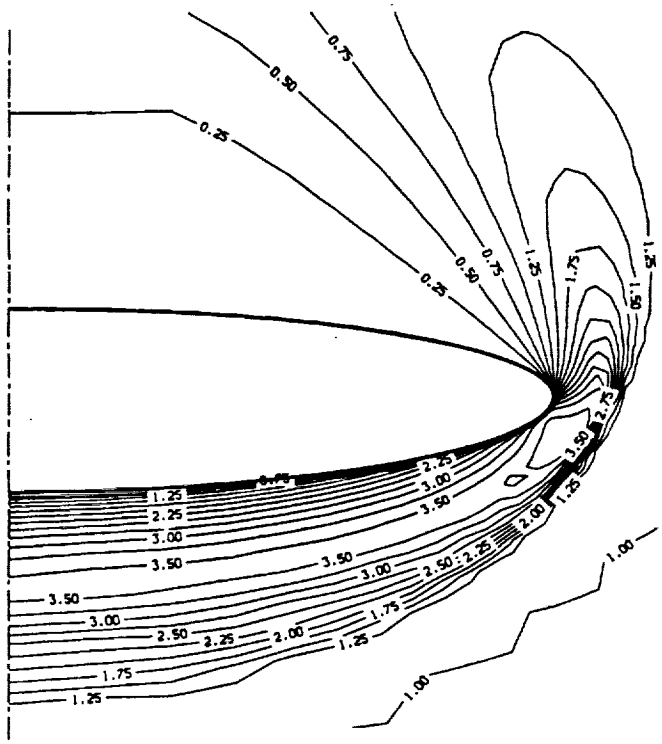

(d) 73% chord

Fig. 6 Isobars, no transpiration, free-stream pressure = 1

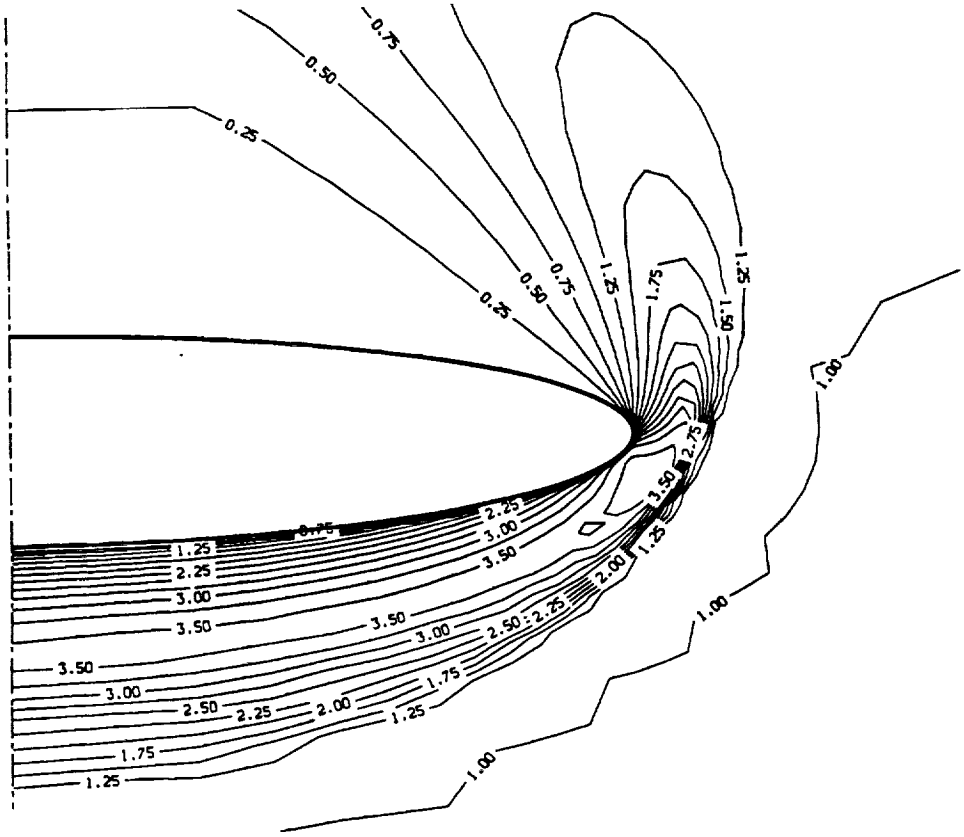

(a)

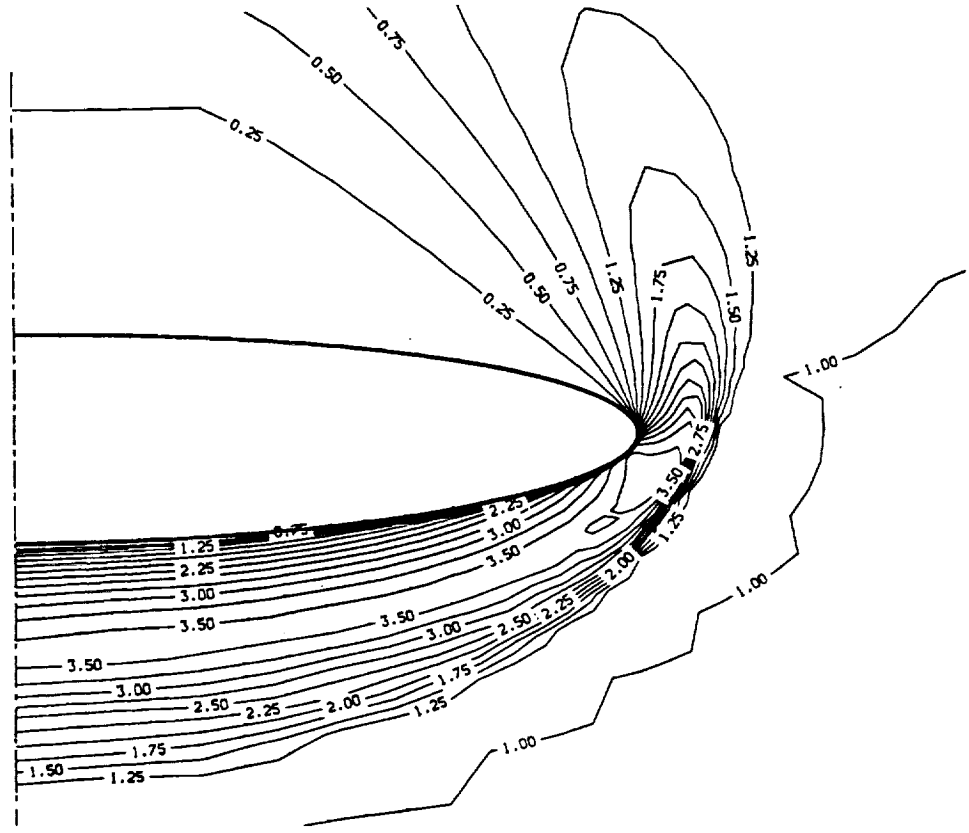

(b)

Fig. 7 Isobars, 73% chord
(a) no transpiration,
(b) transpiration with k = 0.25, outer 17% of span

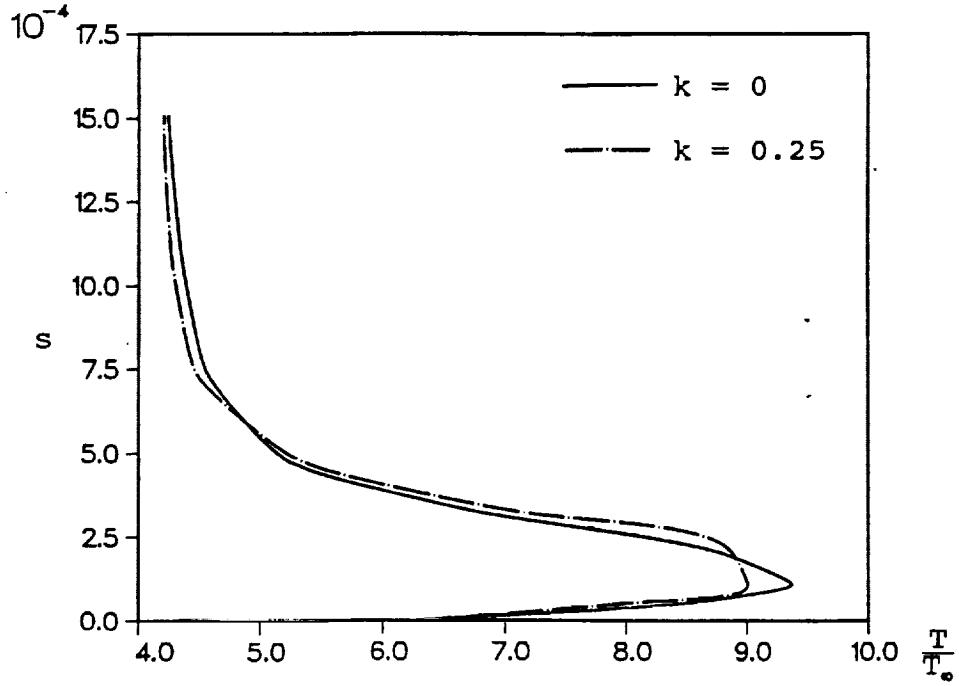

(a) Thermal boundary layer

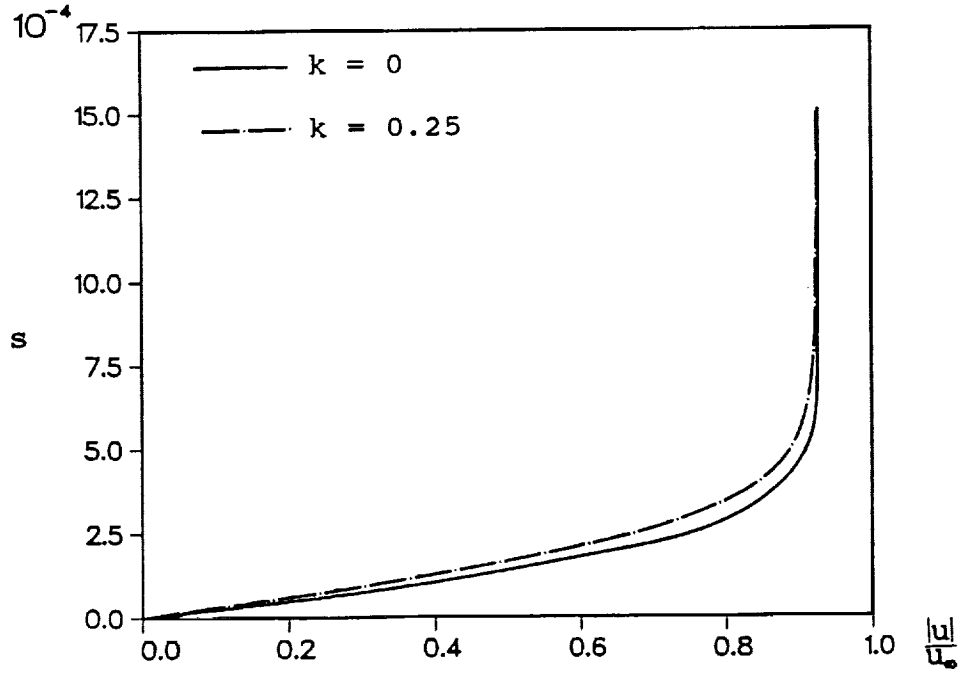

(b) Velocity boundary layer

Fig. 8 Boundary layer at hotest location 50% chord, 98% span.

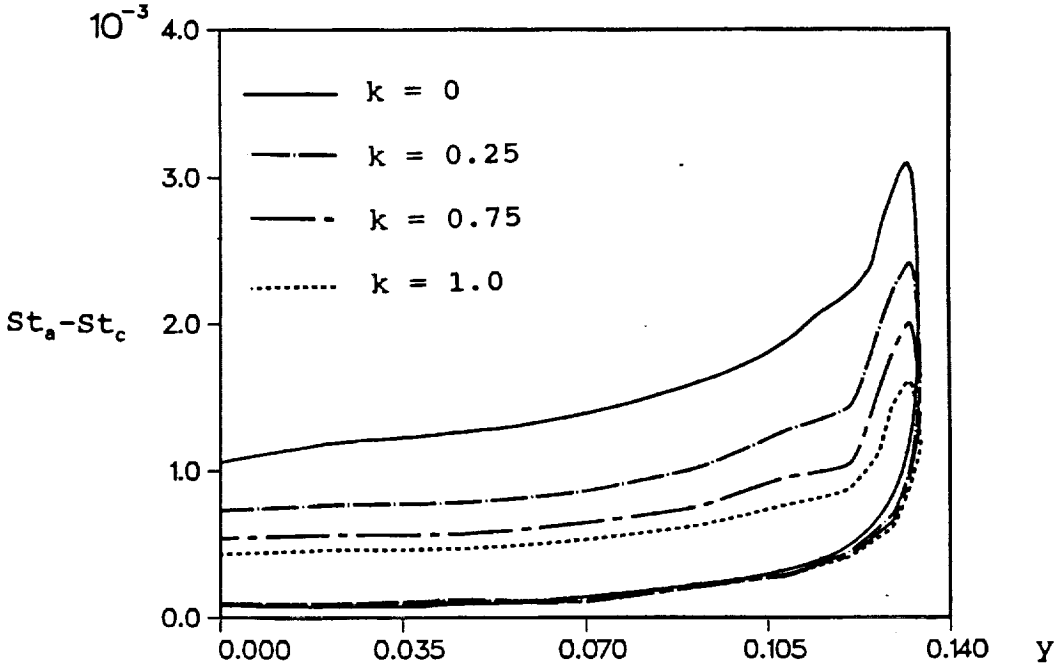

(a) Transpiration over entire lower surface

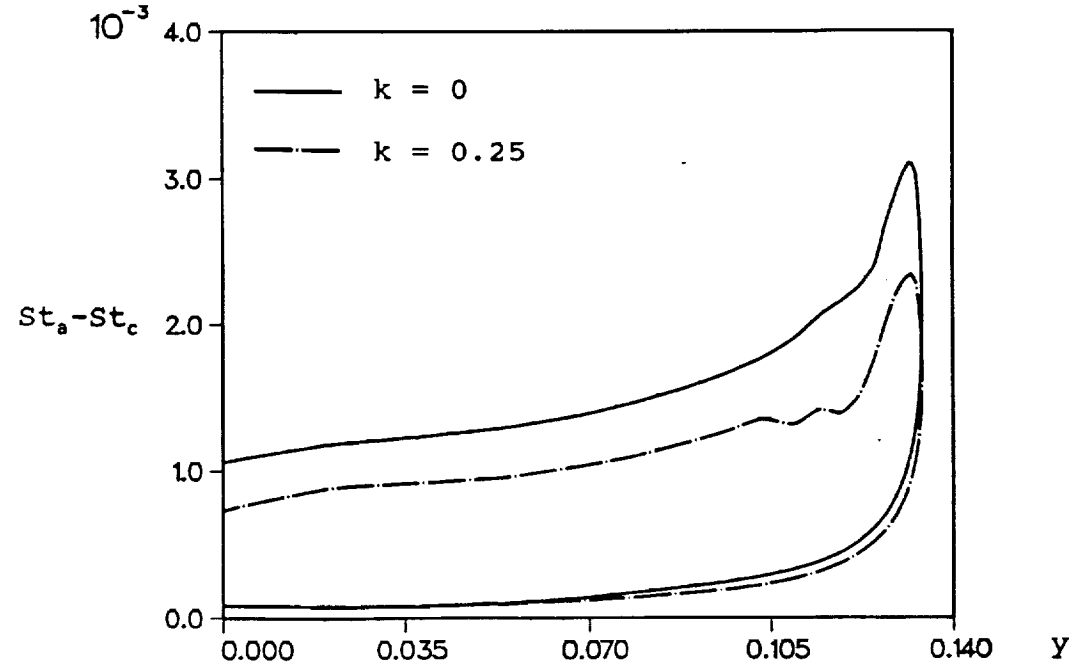

(b) Transpiration over outer 17% of span

Fig. 9 Aerodynamic heating, 50% chord, M = 10.3, Re = 5 10^6, T_w = 1366°K, T_∞ = 218 °K

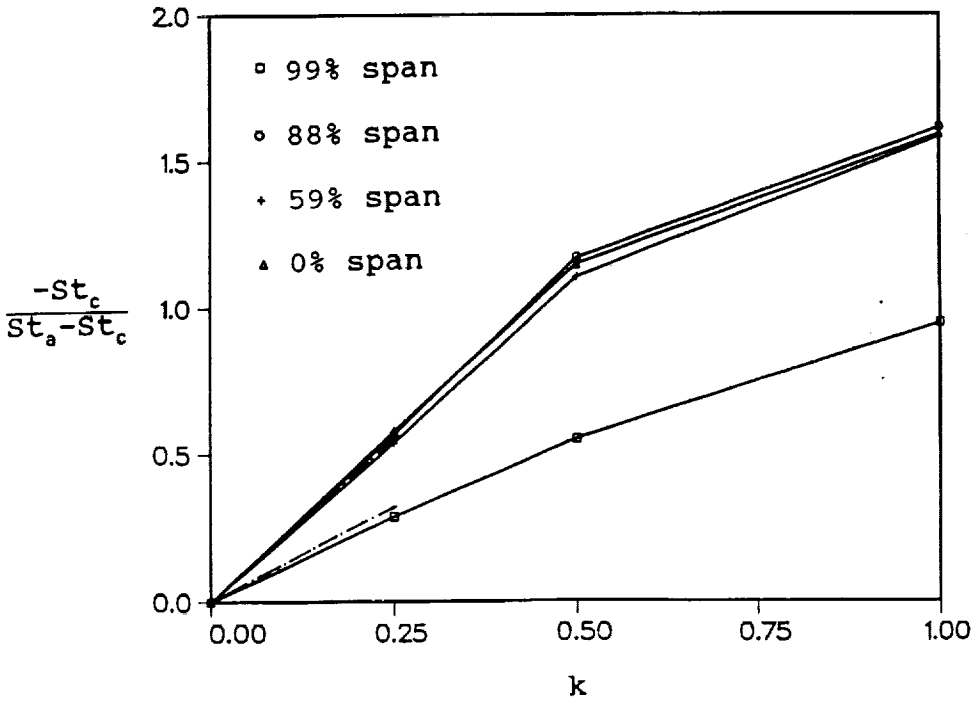

Fig. 10 Relative convective heat dissipation,
solid line: transpiration over entire lower surface
dashed line: transpiration over outer 17% span

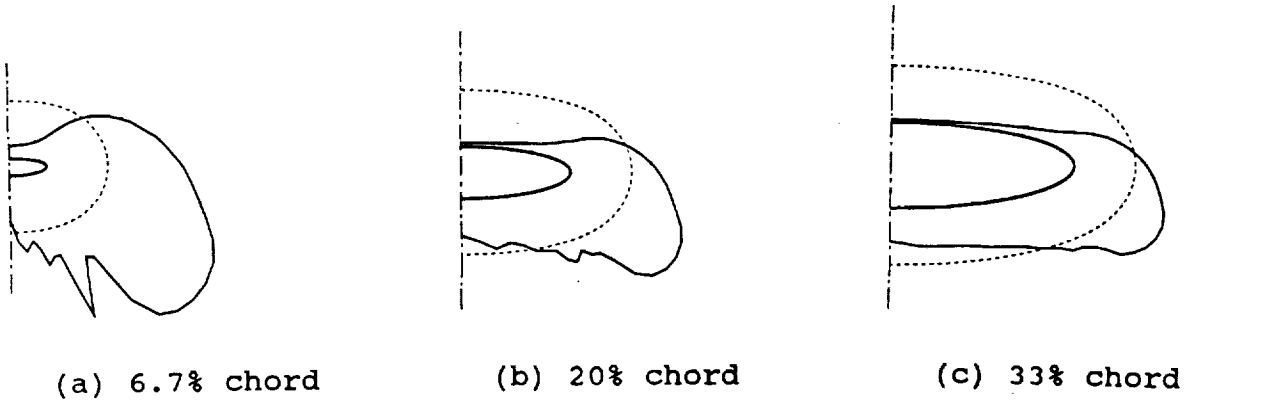

(a) 6.7% chord (b) 20% chord (c) 33% chord

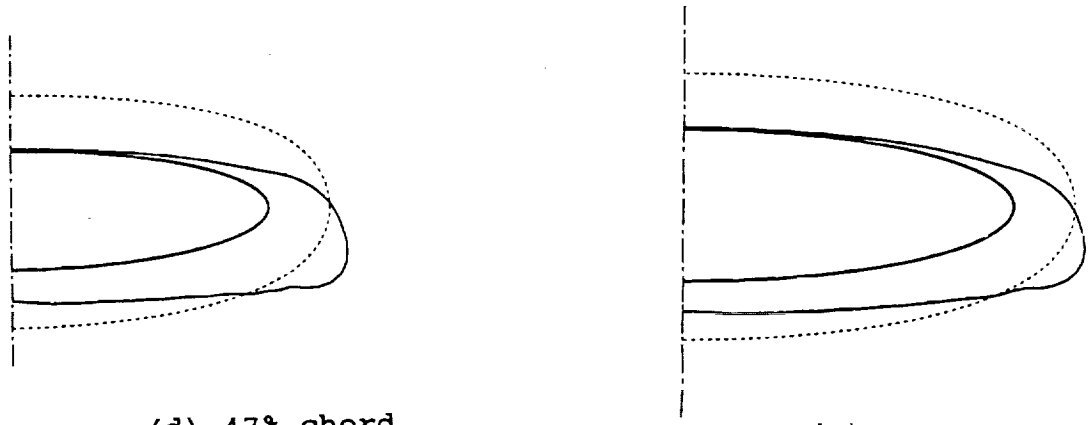

(d) 47% chord (e) 60% chord

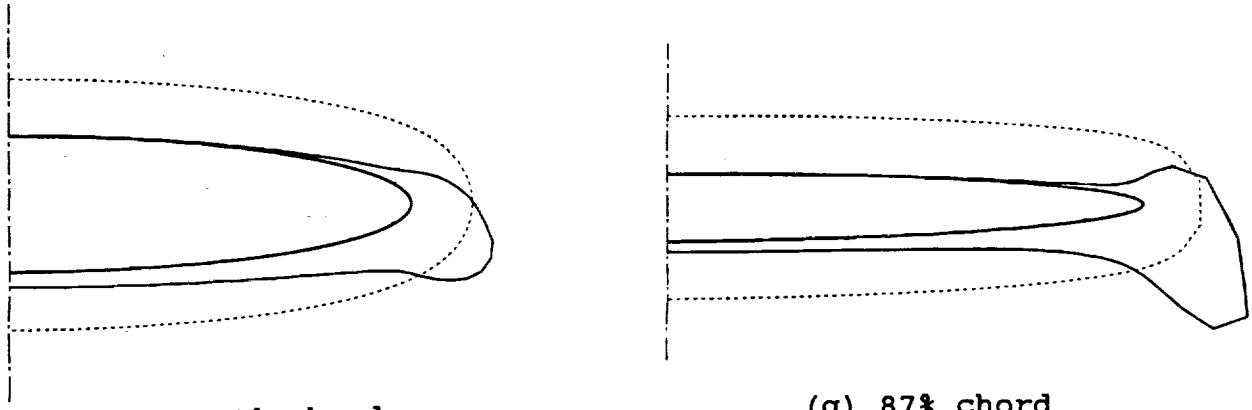

(f) 73% chord (g) 87% chord

Fig. 11 Aerodynamic heating, M = 10.3, Re = 5 10^6, T_w = 1366°K, T_∞ = 218 °K
dashed line represents St_s = 0.002

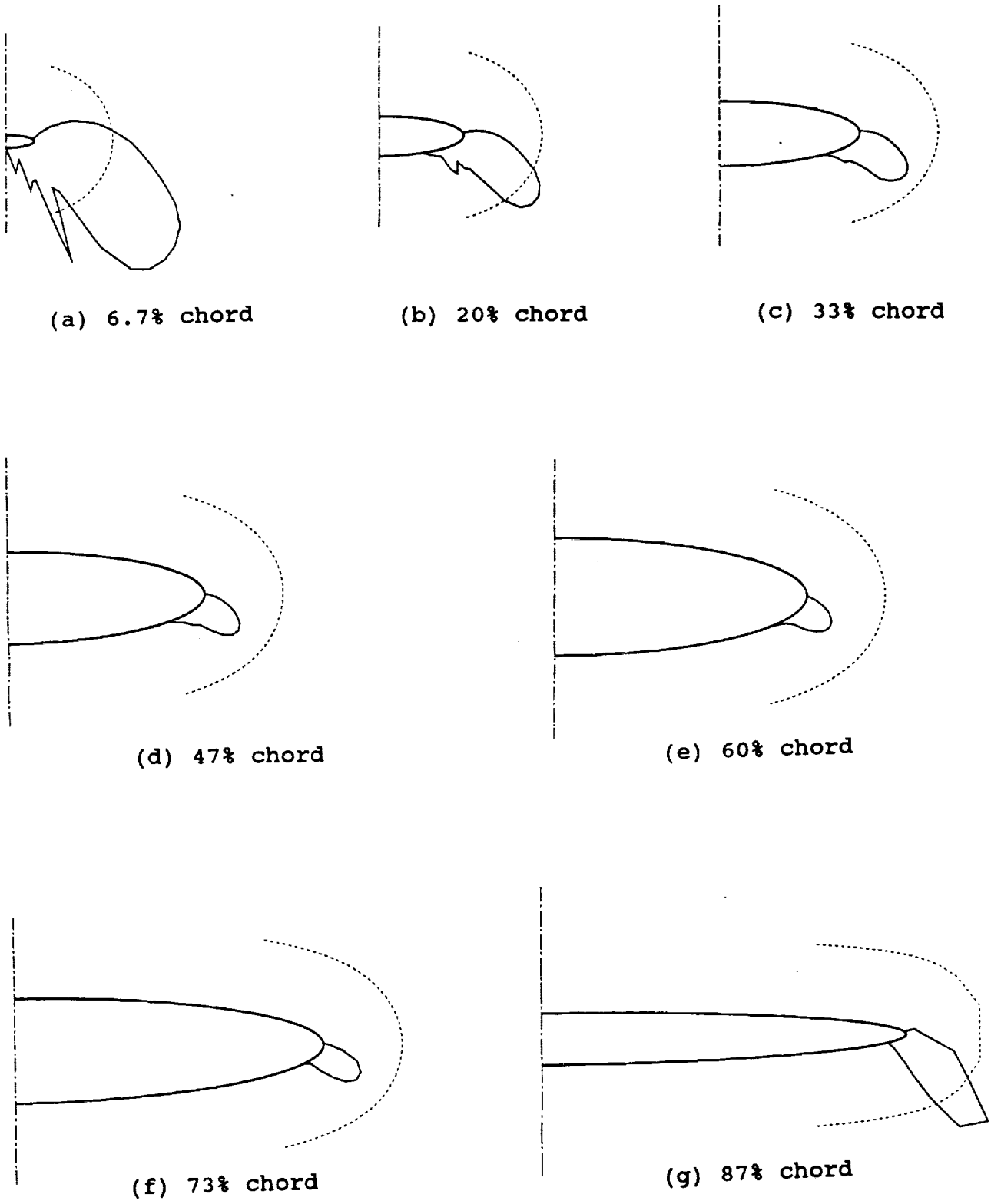

Fig. 12 Value of k to dissipate St_s exceeding 0.002, $M = 10.3$, $Re = 5\ 10^6$, $T_w = 1366°K$, $T_\infty = 218\ °K$ dashed line represents $k = 1$

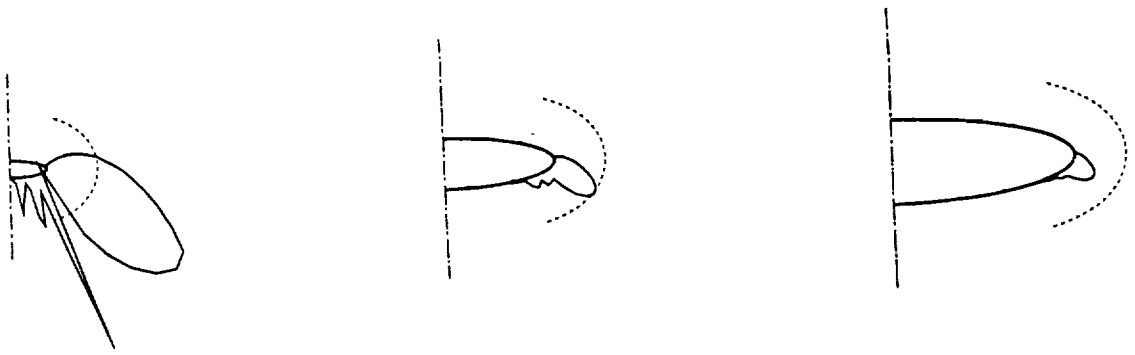

(a) 6.7% chord (b) 20% chord (c) 33% chord

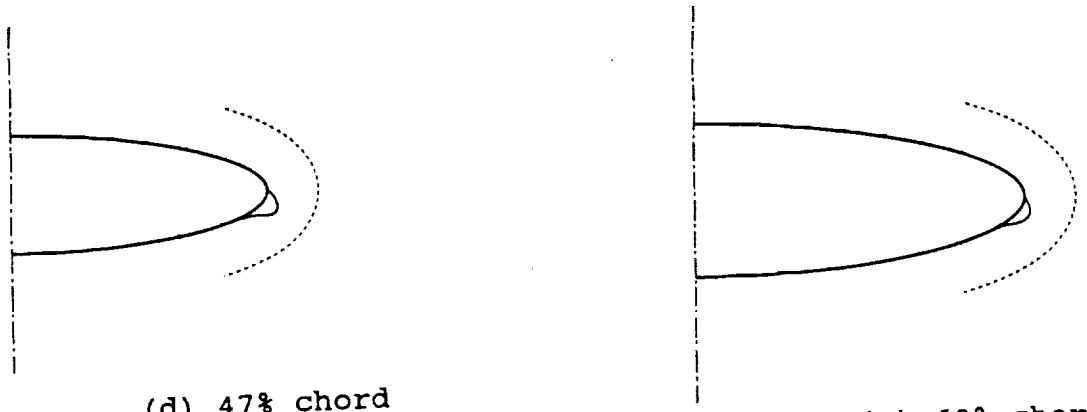

(d) 47% chord (e) 60% chord

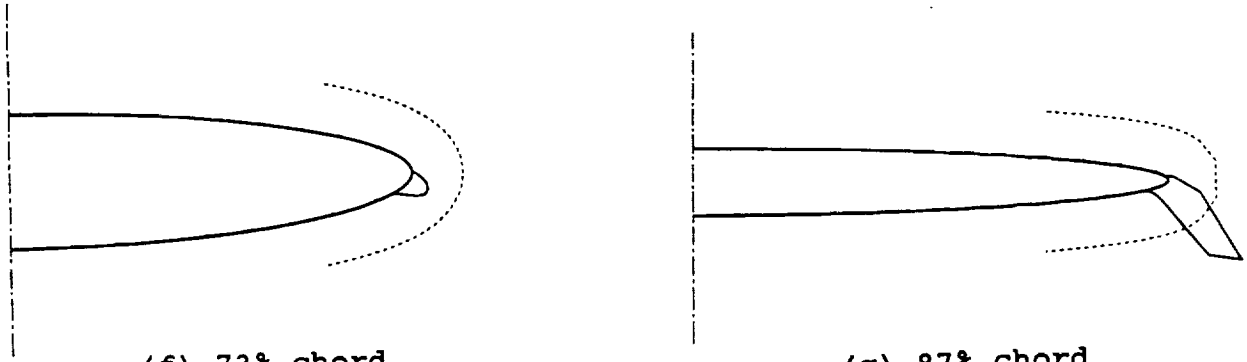

(f) 73% chord (g) 87% chord

Fig. 13 Non-dimensional transpiration intensity corresponding to the k-distribution of Fig. 12
dashed line represents $\bar{\rho}_b \bar{u}_b = 0.005$

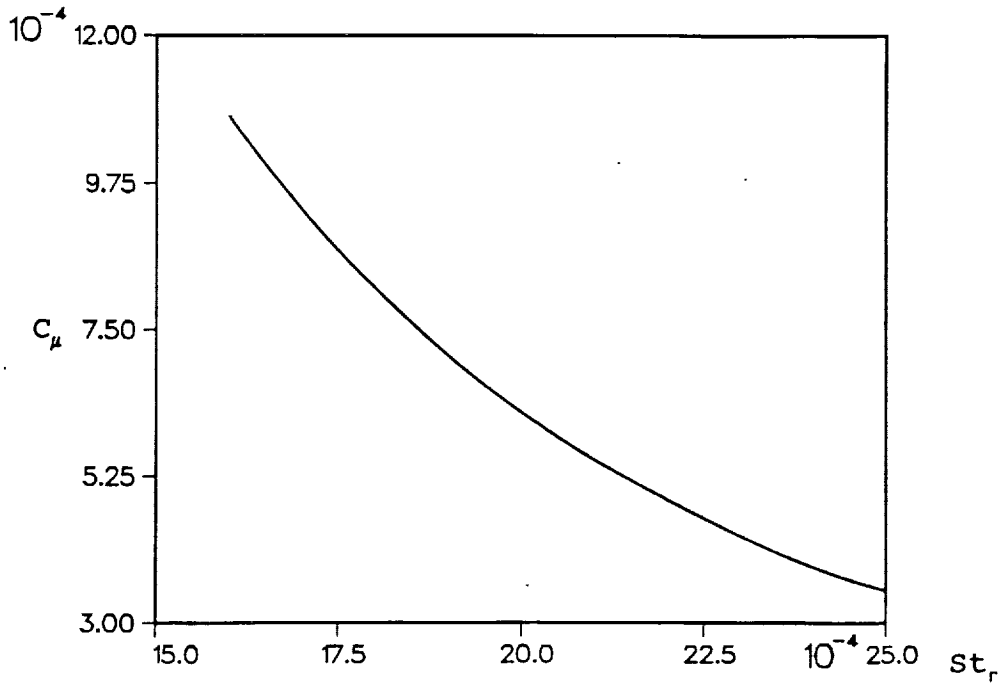

(a)

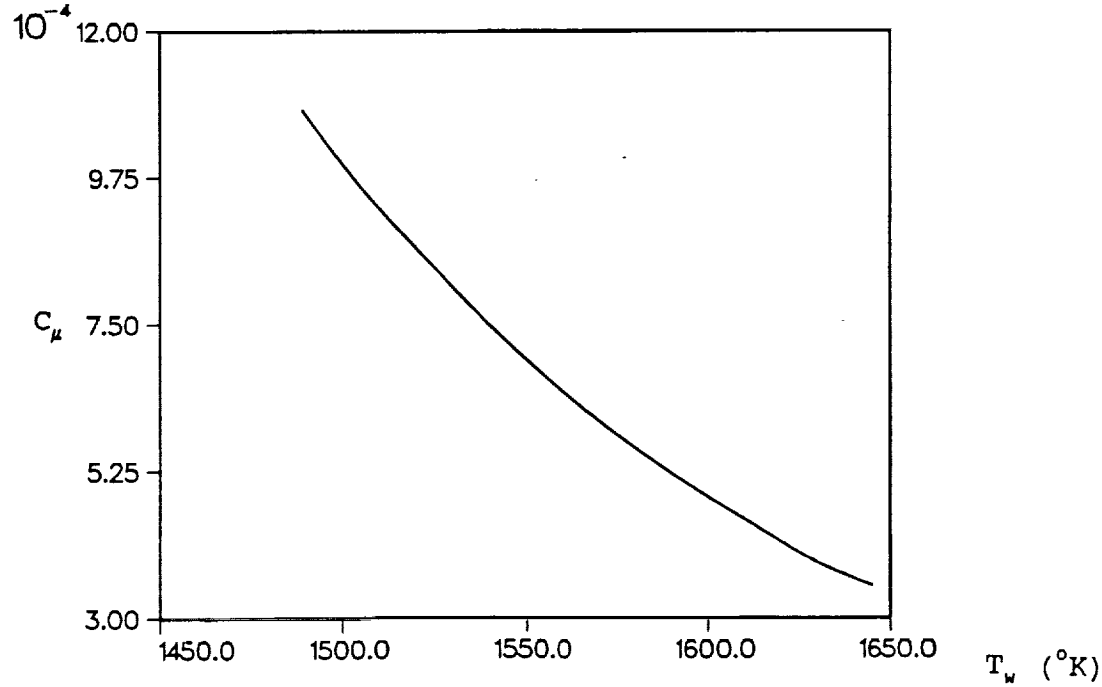

(b)

Fig. 14 Transpiration coefficient